Meteorological Drought Analysis Using Global Climate Model and Drought Indicators in West of Iran

Mahsa Pakdin (mahsapakdin@yahoo.com)
Semnan University https://orcid.org/0000-0003-1806-7513
Morteza Akbari
Ferdowsi University of Mashhad
Mohamad Alizadeh Noughani
Ferdowsi University of Mashhad

Research Article

Keywords: Climate change, LARS-WG, Representative Concentration Pathways, SPEI Index

Posted Date: December 30th, 2021

DOI: https://doi.org/10.21203/rs.3.rs-1100146/v1

Abstract

Climate change and global warming impact the frequency of droughts and supply systems. Therefore, it is necessary to conduct appropriate studies to evaluate the impact of climate change on weather patterns and drought. For this purpose, data from 6 synoptic stations located in the wet and temperate areas in the Zagros region in western Iran were used to construct four general atmospheric models including BCC-CSM1, CANESM2, HADGEM2-ES, NORESM1-M under representative concentration pathways (RCPs) 2.6, 4.5, and 8.5, for three future periods (2010-2039), (2040-2069) and (2070-2099). Then, spatio-temporal variations of drought severity and frequency were studied in the study area using SPI and SPEI indices in different periods up to 2100. The results showed the spatial extent of areas classified as extremely dry will increase by 47.9% in the first period compared to the base period. In the second and third periods, however, the severely dry class covers more area. Analysis of SPEI showed that drought will be more severe in all future periods. According to SPEI, drought frequency will increase by 2% according to the first period (2010-2039) relative to the base period (1984-2013), and by 0.3% in the second and third periods by 2099. The results of this study indicate that the severity, frequency, and impacts of drought will increase in the study area until the end of the century. Therefore, appropriate measures should be taken to control and reduce its potential effects in the future.

1 Introduction

Climate change is one of the most important challenges facing humans and natural ecosystems, bringing about consequences such as the elevated occurrence of atmospheric-climatic hazards, increased number of storm events, reduced yield of crops and orchards, and lowered food security, as well as increased migration from areas facing more severe climate change (Chanapathi 2020; Memarian and Akbari 2021). Drought influences different parts of an ecosystem on different scales. Studies show that in some regions of the world, climate change has triggered droughts, intensified its damaging effects, or created conditions for subsequent droughts. Droughts occur naturally, but climate change has generally accelerated the contributing hydrological processes, making them less gradual and more intense, with many consequences, not the least of which is increased wildfire risk. Different types of drought are being studied, such as meteorological, agricultural, hydrological, and socioeconomic droughts; however, a lack of unanimous definition complicates the study of droughts (Tang 2020; Mukherjee et al. 2018; Haile et al. 2020). According to the Hydrological definition, droughts are extreme hydrological phenomena that are characterized by a long-term lack of precipitation in a vast area, in any climatic condition (Taxak et al. 2014; Akbari et al. 2016).

Various scenarios for the increase in greenhouse gases have been defined in terms of general circulation patterns of the atmosphere to predict climate change. Since the spatial accuracy of general circulation models is very low and the effects of variations have limited applicability, these models need to be converted for smaller spatial scales, which are referred to as the "scalar" model. In general, there are two methods for the conversion of general circulation models for finer scales: dynamic and statistical methods, in addition to combinations of both. Many different approaches have been proposed to carry out these conversions, the most reliable of which is the use of coupled AOGCM simulations, integrating (coupling) global climate models (GCMs) and regional climate models (RCMs) to enable the study of climate change over time in different parts of the world (Semenov 2009; IPCC 2007,2013; Fang et al. 2018; Kang et al. 2019). The LARS-WG model is a randomized weather generator that is used to simulate climatic data at a specific station under the current and future conditions influenced by the climate change phenomenon. So far, many studies have been conducted on the LARS-WG model (Khan et al. 2006; Wilby and Harris 2006; Pakdin et al. 2021).

Drought monitoring has helped many users and organizations by capturing the characteristics of droughts using droughts indexes. More than 100 drought indexes have been suggested so far, some of which have been used to describe drought characteristics in grid maps at regional and national scales (Zargar et al. 2011; Valavi et al. 2019; Shiravand 2020). Extensive research has been done on the effects of climate change on drought through the use of drought indexes (Vicente-Serrano et al. 2010; Zhou et al. 2014; Dubrovsky et al. 2008; Caccamo et al. 2011). (Pelt and Swart 2011) used SPEI in the Czech Republic and emphasized the ability of this index to recognize the severity of drought. (Stagge et al. 2015) compared the distribution of SPI and SPEI drought indices in Europe. Their results identified the gamma distributions and the general limit values for SPI and SPEI, respectively. (Lee et al. 2017) studied the effects of climate change on drought using SPEI in North Korea from 1981 to 2100. Their results indicated that SPEI will change from -0.9 in 1995, to 1.18 in 2025. Given Iran's geographical location in an arid region, research has been done to predict droughts and their impact on the country (Haile et al. 2020; Bąk and Kubiak-Wójcicka 2017; Lweendo et al. 2017). The Zagros region (a large region in the west of Iran), has been subjected to tensions due to lack of precipitation, which has led to the depletion of the region and serious socio-economic problems. Although some studies have utilized different models to assess climate change and drought in the region, few have combined different models with climate change scenarios for meteorological analysis of droughts. Therefore, we assessed the impact of climate change on drought in the Zagros region of Iran using four general circulation models, under three climate change scenarios. Also, the Standardized Precipitation Index (SPI) and the Standardized Precipitation Evapotranspiration Index (SPEI) were calculated for future periods. In this work, we 1-examine the variation in SPI and SPEI to describe variation in drought characteristics in the Zagros region, 2-evaluate the impact of climate change on drought characteristics, 3-predict drought severity by 2099, and 4-investigate the spatial distribution of changes in drought patterns.

2 Materials And Methods

2.1 Study area

The Zagros climatic zone covers Iran from the northwest to the southwest (Fig. 1). The region has a temperate and humid climate characterized by seasonal precipitation. According to the climatic classification of (Alijani 1999), the regions consist of three climate classes: sub-humid subtropical, cold, and semi-mountainous areas. The average annual precipitation (P) varies between 250 and 800 mm in different parts of the region. Rainfall historically occurs during winter and spring. Summers are hot and dry (mean temperature: 35 ºC) and winters are cool (mean temperature: 7 ºC) (Fathizadeh et al. 2013). Past studies show that only six synoptic stations in the area have data with adequate quality for this research. Table 1 shows the characteristics of these stations.

Table 1
The synoptic stations used in the study (data from Iranian Meteorological Organization)

Station	Longitude	Latitude	Elevation (m)
Sanandaj	47.01	35.25	1373.4
Kermanshah	47.15	34.35	1318.5
Shahrekord	50.84	32.29	2048.9
Shiraz	52.63	29.56	1488
Fasa	53.72	28.90	1268
Khorramabad	48.40	33.43	1147.8

2.2 Dataset

Minimum temperature, maximum temperature, irradiation, and precipitation data were obtained daily from six synoptic stations in the Zagros region. The common statistical basis was considered from 1984 to 2013, and pre-processing of data took place.

2.3 Downscaling statistical data

For this purpose, past and future climates at the six stations were simulated. The basic requirement of the model at the calibration stage is a file that identifies past climate at the stations (Semenov and Stratonovitch 2010). This file was compiled using daily precipitation data, minimum temperature, maximum temperature, and irradiance at synoptic stations, taking 1984-2013 as the base period. According to the latest IPCC recommendation, the use of multiple models in climatic simulations, instead of running the models individually, can be effective in reducing the uncertainties in the model. To that end, we used four GCMs (BCC-CSM1, CANESM2, HADGEM2-ES, NORESM1-M, Table 2), and three representative concentration pathways (RCP 2.6, 4.5, and 8.5), and calculated the arithmetic mean for each group in R. Finally, precipitation, minimum temperature, maximum temperature, and irradiance were projected for future periods (2010-2039) and (2040-2069) and (2070-2099).

Table 2
List of GCMs in IPCC AR5 (Miao et al, 2014)

GCM	Model	Resolution	Source
BCC-CSM1	It is a fully coupled global climate-carbon model including interactive vegetation and the global carbon cycle in which the atmospheric component, ocean component, land component, and sea ice component are fully coupled and interact with each other through fluxes of momentum, energy, water, and carbon at their interfaces. The exchange of atmospheric carbon with the land biosphere is calculated at each model time step (20 min).	160 × 320	Beijing Climate Center, China Meteorological Administration, China
CanESM2	This is the fourth generation of the atmospheric-ocean public circulation model. There are 40 vertical levels with a distance of 10 meters near the surface (there are 16 levels at a height of 200 meters) to nearly 400 meters deep in the ocean. Spherical horizontal coordinates are used with lattice distance ~ 1.41 ° latitude and 0.94 ° latitude.	64 × 128	National Center for Atmospheric Research (NCAR), United States
HadGEM2-ES	The HadGEM2-ES is a coupled ground system model used by the Hadley Met Office to simulate CMIP5. The HadGEM2-ES climatic model includes an atmospheric GCM with a horizontal and vertical resolution of N96 and L38 and an oceanic GCM with a horizontal resolution of 1 degree (rising to 3.1 degrees at the equator) and 40 vertical levels.	145 × 192	Met Office Hadley Center, Unites Kingdom
NorESM	The Norwegian Ground System Model (NorESM) is one of 20 climate models producing output for the NorESM1-M CMIP5, with a horizontal resolution of ~ 2 ° for atmospheric and terrestrial components and 1 ° for the ocean and ice components.	96 × 144	Norwegian Climate Centre, Norway

2.4 Standardized Precipitation Index (SPI)

The standardized precipitation index is one of the most important indices in drought monitoring. This index is one of the few time-sensitive drought indices. SPI allows for determining the time scale, depending on which aspects of the impact of droughts are more important (e.g., agricultural resources, hydrological features, etc.). The time scale can range from one month to several years. Also, there are more indicators available for analyzing the severity, duration, and frequency of drought using SPI compared to other indexes (Huang et al. 2016; Lin et al. 2020; Nabaei et al. 2019; Gebrewahid et al. 2017; Teuling et al. 2013; Won et al. 2018). In this study, the time scale was set to one year. Only the precipitation parameter is used in the calculation of SPI. The precipitation of each station is calculated on the timescale. Table 3 shows the classification of SPI and SPEI indices according to (McKee 1995).

Table 3
The Classification of SPI and SPEI indices (McKee, 1995)

Extremely Wet	Very wet	Moderately Wet	Normal Wet	Normal Dry	Moderately Dry	Severely Dry	Extremely Dry
+2.0	1.5-1.99	1.0-.149	-0.99-0	0-0.99	-1.0- -1.4	-1.5–1.99	-2.0 or less

2.5 Standardized Precipitation Evapotranspiration Index (SPEI)

SPEI was first introduced by (Serrano et al. 2010). This index is a multivariate index in which precipitation data and evapotranspiration data are combined. This index is calculated similarly to the standardized precipitation index. However, SPI utilizes monthly precipitation, while SPEI utilizes monthly precipitation difference and potential

evapotranspiration (PET), representing climate water balance. SPEI has been widely used to study meteorological droughts (Chen et al. 2015; Shao et al. 2018; Paulo et al. 2012; Ren et al. 2012; Wang et al. 2015; Wolf et al. 2011; Yao et al. 2018; Zhao et al. 2015). Table 3 presents how this index is classified. In this study, SPEI was calculated on a one-year time scale in R.

SPEI is derived from equations (1) to (7):

$$m = 6.75 \times 10^{-7} I^3 - 7.71 \times 10^{-5} I^2 + 1.79 \times 10^{-2} I$$

1

$$PET = 16K\left(\frac{10T}{I}\right)^m$$

2

$i = \left(\frac{T}{5}\right)^{1.514}$(3)

$$K = \left(\frac{N}{12}\right)\left(\frac{NDM}{30}\right)(4)$$

Where T is the average monthly temperature in Celsius, m is the coefficient of dependence on I, I is the sum of 12-month heat indexes, k is the correction factor in terms of month and latitude, NDM is the number of days in a month, and N is the maximum number of hours of sunlight. Thus, with a value for *PET*, the difference between the precipitation (*P*) and *PET* for the month *i* is calculated:

$$\mathrm{D_i} = \mathrm{P_i} - \mathrm{PET_i}$$

5

The calculation of SPEI requires a three-parameter distribution. The probability distribution function of series D is based on the following equation:

$$F(x) = \left[1 + \left(\frac{\alpha}{x - y}\right)^{\beta}\right]^{-1}$$

6

Where, α, β and x are the parameters of scale, shape and position for D values (Singh et al. 1993). The values of F(x) for series D in different time scales are well suited to the observed experimental values, so SPEI can be simply calculated from the standard values of F (x).

$SPEI = W - (C_0 + C_1 W + C_2 W^2 / 1 + d_1 w + d_2 w^2 + d_3 w^2)$ (7)

Where $W = \sqrt{2\ln(\mathrm{P})}$ for $P \leq 0.5$, P being the probability of higher values of D is determined. The values of C_0, C_1 and C_2 and also d_1, d_2 and d_3 are fixed. The mean value of SPEI is zero and the standard deviation is equal to one. SPEI is a standardized variable, so it can be compared with other SPEI values from different places and times. A SPEI value of zero is equivalent to the 50% cumulative probability D (Mavromatis 2007).

2.6 Kernel smoothing method

The kernel smoothing method provides promising results for two simulated and one real-world data set. At the same time, it offers a great alternative for Kriging approaches, in particular in cases where the estimation process has failed. This can be the case when either there are few samples or the observed data are not suitably designed for computer experiments. In this condition, the working unit is a polygon created through Delaunay triangulation. The approach is flexible enough to embed different types of kernel and weight functions. As the method can be easily executed, it can be used as a criterion to validate other interpolation methods (Muhlenst 2009). This method has been used in past studies such as (Hessl et al. 2018; Xu et al. 2020).

Kernel smoothing can be a good option given noisy measurements $x(t_i)$ of processes at irregularly spaced times t_i. The smoother is a weighted average (Eqs 8 and 9).

$$\mathrm{x}\left(\mathrm{t}\right)=\frac{\sum_{\mathrm{i}=1}^{\mathrm{N}}\mathrm{K}\left(\mathrm{t}-\mathrm{ti}\right)\mathrm{x}\left(\mathrm{ti}\right)}{\sum_{\mathrm{i}=1}^{\mathrm{N}}\mathrm{K}\left(\mathrm{t}-\mathrm{ti}\right)}$$

8

$$K\left(T\right)=\exp\left(-\frac{T^2}{2\tau^2}\right)$$

9

3 Results

LARS-WG is one of the most commonly applied weather generators, in which the meteorological data for the future period are generated by considering temperature and precipitation alterations under the climate scenarios of RCP 2.6, 4.5 and 8.5. According to the obtained SPI values, droughts will increase in the eastern and northern parts of the regions, while the opposite will take place in the western part of the region. However, SPEI shows that drought will increase from the center of the region to the west. Overall, drought will increase in the entire region by about 11-15% compared to the base period.

SPI and SPEI were used to study temporal and spatial changes of drought severity and frequency in the Zagros region in different periods until 2099. SPI shows that although the spatial extent of drought increases significantly in the first period compared to the base period (47.9%), in the second and third periods of the drought compared with the base period, dry classes have a much larger area. However, SPEI indicates the spatial dominance of drought with very high intensity in all periods. A general review of the results indicates an increase in the frequency and severity of drought as well as the development of drought-affected areas by the end of the century. Therefore, it is necessary to take appropriate measures to reduce the potential effects of climate change on different ecosystems in the region.

3.1 Impact of climate change on drought based on SPI

The standardized precipitation index (SPI) depends on precipitation as a single variable, while the standardized precipitation evapotranspiration index (SPEI) is obtained from precipitation and temperature in the form of a simple water balance. Both indicators detected changes in the frequency of drought in the future compared to the base period. SPI and SPEI agreed on the direction of change, but showed different effects for climate change on drought

conditions. SPI is useful because it only needs rainfall as input. However, the use of SPI to describe drought should be done with caution. According to Table 4, normal dry and normal wet classes are the most frequent. The extremely wet class has the lowest frequency (17.7 month). On the whole, more than 7% of the month in the base period (1984-2013) were categorized in the severely dry and extremely dry classes.

Table 4
Frequency of SPI classes during the base period (1984-2013)

Stations	Extremely dry	Severely dry	Moderately dry	Normal dry	Normal wet	Moderately wet	Very wet	Extremely wet
Sanandaj	13	17	22	134	114	34	16	10
Kermanshah	11	19	19	126	137	24	18	6
Khorramabad	3	30	27	127	113	39	8	13
Shahrekord	10	16	47	75	163	24	25	0
Shiraz	12	14	29	118	122	41	20	4
Fasa	4	11	32	163	83	21	36	10
Average	8.83	17.83	29.33	123.8	122	30.5	20.5	17.7
percentage	2.45	4.95	8.15	34.40	33.89	8.47	5.69	1.99

3.1.1 Changes in the first period compared with the base period

Our analysis showed that the frequency of drought in the first period will increase by 28% compared to the base period, while the frequency of wet classes will increase by 0.35%. Normal classes (both wet and dry) were unchanged, and the largest difference was observed for the dry classes with an increase of about 9.23% (As shown in Tables 4 and 5).

Table 5
Frequency of SPI classes during the first period (2010-2039)

Stations	Extremely dry	Severely dry	Moderately dry	Normal dry	Normal wet	Moderately wet	Very wet	Extremely wet
Sanandaj	11	20	23	104	156	24	15	7
Kermanshah	13	14	25	130	100	53	20	5
Khorramabad	5	22	32	110	140	43	2	6
Shahrekord	7	22	33	113	119	41	22	3
Shiraz	3	2	40	98	120	55	13	3
Fasa	11	18	15	145	119	25	16	11
Average	8.33	20.67	28.00	116.6	125.67	40.17	14.6	5.83
Percentage	2.31	5.74	7.78	32.41	34.91	11.16	4.07	1.62

3.2.2 Changes in the second period compared with the base period

The result showed the frequency of drought will increase by 4.78% compared to the base period, and the wet period will decrease by 7.7% the percentage of changes in the normal classes has decreased by 1.41%. Among the stations, Sanandaj shows the largest change in the occurrence of dry periods with an increase of 84.88% compared to the base period (Tables 4 and 6).

Table 6
Frequency of SPI classes during the second period (2040-2069)

Stations	Extremely dry	Severely dry	Moderately dry	Normal dry	Normal wet	Moderately wet	Very wet	Extremely wet
Sanandaj	13	19	35	84	165	27	10	7
Kermanshah	13	13	20	136	120	34	19	5
Khorramabad	7	17	32	113	146	26	11	8
Shahrekord	2	27	34	114	118	41	21	3
Shiraz	2	21	41	102	123	52	15	4
Fasa	12	15	29	139	124	13	18	10
Average	8.17	18.67	31.83	114.6	132.6	32.17	15.6	6.17
Percentage	2.27	5.19	8.84	31.85	36.85	8.94	4.35	1.71

3.2.3 Changes in the third period compared with the base period

Dry periods will increase in the third period by 0.9% compared to the base period, and the wet period is 18.8%. The frequency of dry classes is expected to increase by 56.1%. Fasa station will have a significant increase in the incidence of drought compared to the base period (Tables 4 and 7).

Table7 Frequency of SPI classes during the third period (2070-2099)

Stations	Extremely dry	Severely dry	Moderately dry	Normal dry	Normal wet	Moderately wet	Very wet	Extremely wet
Sanandaj	15	13	31	106	150	28	15	2
Kermanshah	13	13	18	138	121	33	19	5
Khorramabad	5	37	14	102	141	44	16	1
Shahrekord	3	23	41	97	144	35	14	33
Shiraz	2	25	35	107	118	57	15	1
Fasa	11	15	25	138	136	6	18	11
Average	8.17	21	27.33	114.67	135	33.83	16.1	3.83
Percentage	2.27	5.83	7.59	31.85	37.50	9.40	4.49	1.06

3.3 Spatial changes in SPI

The frequency of three levels of the drought was calculated and their spatial variations were plotted using kernel smoothing. (Fig. 3) shows the percentage of the study area covered by each class. In the base period, the

northeastern and central parts of the study area experienced the most severe droughts, with all three classes having roughly the same area (Fig. 2 and Fig. 3). As we move from the northeast to the northwest and from north to south, we see an increase in drought at synoptic stations, which is consistent with the results of other studies (Abbasi et al. 2019; Mirzayi Hasanlo et al.2020; Fathian et al. 2017). The most severe drought is seen in the eastern part of the region, followed by the western, northern, and southern regions. Also, projected maps in the region show an increase in droughts in the northern parts and a decrease in the southern part.

In the first period (2010-2039), the most severe droughts are expected in the central and northeastern parts of the region and the least severe droughts in the southeastern parts. In this period, the severity of droughts will increase, so that about half of the region will be exposed to very severe drought. In the second period (2040-2069), drought is projected to occur in the north. On the other hand, the southeastern and southwestern parts are less likely to experience severe drought. The severely dry class will cover more than half of the region in this period. In the third period (2070-2099), drought is projected mainly in the northeast. The extent of areas in the severely dry class will increase compared to the base period, but coverage will decrease for the moderately dry class.

3.4 Impact of climate change on drought based on SPEI

Extremely dry and severely dry droughts identified by SPEI are generally more severe than those identified by SPI in terms of affected area and duration.

Table 8
Frequency of SPEI classes during the base period (1984-2013)

Stations	Extremely dry	Severely dry	Moderately dry	Normal dry	Normal wet	Moderately wet	Very wet	Extremely wet
Sanandaj	4	28	20	147	101	28	26	66
Kermanshah	2	27	23	126	111	39	28	4
Khorramabad	5	18	39	135	98	39	15	11
Shahrekord	6	19	41	132	108	26	21	7
Shiraz	12	9	25	157	94	26	35	2
Fasa	12	12	17	175	70	29	43	2
Average	6.83	18.83	27.50	145.33	97	31.17	28	5.33
Percentage	1.90	5.23	7.64	40.37	26.94	8.66	7.78	1.48

3.4.1 Changes in the first period compared with the base period

Projected SPEI showed that the frequency of droughts will increase by 11.9% in the first period compared to the base period, and that the frequency of wet months will decrease by 6%. The frequency of normal dry and normal wet months showed a 1% decrease. Shiraz station will experience the greatest increase in dry periods (52%) compared to baseline (Tables 8 and 9).

Table 9
Frequency of SPEI classes during the first period (2010-2039)

Stations	Extremely dry	Severely dry	Moderately dry	Normal dry	Normal wet	Moderately wet	Very wet	Extremely wet
Sanandaj	6	25	29	124	125	23	23	5
Kermanshah	3	21	25	136	114	34	24	3
Khorramabad	2	21	40	115	126	39	13	4
Shahrekord	0	22	36	126	108	43	25	0
Shiraz	0	24	46	107	110	56	16	1
Fasa	8	15	34	132	115	26	20	10
Average	3.17	21.33	35	123.33	116.33	36.83	20.17	3.83
Percentage	0.88	5.93	9.72	34.26	32.31	10.23	5.60	1.06

3.4.2 Changes in the second period compared with the base period

Results showed that the frequency of drought in the second period will be 12.44% higher than the base period, which is similar to the changes in the first period. Wet periods are also reduced by 1.3%, and the percentage change in the normally dry and normal wet months is expected to be -2.47% (Tables 8 and 10).

Table 10
Frequency of SPEI classes during the second period (2040-2069)

Stations	Extremely dry	Severely dry	Moderately dry	Normal dry	Normal wet	Moderately wet	Very wet	Extremely wet
Sanandaj	3	26	32	109	134	30	17	9
Kermanshah	5	20	29	132	109	36	26	3
Khorramabad	1	21	39	107	139	33	15	5
Shahrekord	1	22	33	125	105	48	26	0
Shiraz	0	21	51	110	103	58	17	0
Fasa	7	15	33	127	119	30	28	1
Average	2.83	20.83	36.17	118.3	118.17	39.17	21.50	3
Percentage	0.79	5.79	10.05	32.87	32.82	10.88	5.97	0.83

3.4.3 Changes in the third period compared with the base period

The frequency of drought will increase by 22% in the third period compared to the base period and wet periods will decrease by 7%. Also, normal dry and normal wet periods will undergo a decrease of 61.3%. At Khorramabad station, significantly compared to the base period, and Sanandaj station will most frequently experience dry periods among the stations, with a large change (23%) in drought months compared to the base period (Tables 8 and 11).

Table 11
Frequency of SPEI classes during the third period (2070-2099)

Stations	Extremely dry	Severely dry	Moderately dry	Normal dry	Normal wet	Moderately wet	Very wet	Extremely wet
Sanandaj	3	26	40	101	138	29	22	1
Kermanshah	5	21	26	136	112	36	27	2
Khorramabad	1	25	43	115	118	34	22	2
Shahrekord	1	22	39	117	125	38	17	1
Shiraz	0	27	45	105	109	56	17	1
Fasa	8	21	36	122	116	28	22	7
Average	3.00	23.67	38.17	115.17	119.67	36.83	21.17	2.33
Percentage	0.83	6.57	10.60	31.99	33.24	10.23	5.88	0.65

3.5 Spatial changes in SPEI

Investigating the spatial extent of changes in SPEI in the base period showed droughts were most frequent in the central and northeastern parts of the region and least frequent in the south of the region (Fig. 4). In the first period, extreme droughts are predicted to occur to the south of the central areas, and the northern parts will experience less severe droughts. The central part of the area is affected by severely dry conditions. The severely dry class will cover nearly half of the region (47.6%) (Fig. 4 and Fig. 5). In the second period, extremely dry conditions are expected in the north and south of the region, and severely dry conditions are predicted from the center towards the north. The severely dry condition will dominate the region with a coverage of 55.4% (Fig. 4 and Fig. 5). In the third period, the northwest will have moderately dry conditions, and the severely dry class will be the most prevalent at 45.25% (Fig. 4 and Fig. 5).

Similar to past studies (Mehr et al. 2019; Tirivarombo et al. 2018; Pei et al. 2020), we observed differences in predictions made using SPI and SPEI. From a time series perspective, the changes in SPI and SPEI at each time scale had some similarities. In short timescales, these two indices had the most fluctuation and the difference between them was the largest. There was a 30% difference between the frequency of drought intensity classes predicted based on SPI and SPEI. Over long timescales, the fluctuations in SPI and SPEI were mild and the differences between them decreased. However, these small changes still led to different classification outputs. Also kernel smoothing Compared to the classical kriging approach, it shows better performance in certain cases of data sets and data with unstable behavior.

4 Discussion And Conclusion

In this study, standardized precipitation index (SPI) and standardized precipitation evapotranspiration index (SPEI) were used to study droughts in the Zagros region of Iran in the past and future. SPI showed that normal classes are predominant in different periods. However, in the SPEI index, this frequency will increase by 2% relative to the first period relative to the base period, and by 0.3% in the second and third periods by 2099. Using SPI, we found that the extremely dry class covers the central and southern parts of the region, and the mildly arid class occupies the northwestern and northeastern parts, with a smaller area. Using SPEI however, it was observed that the extremely dry class will gradually extend to the northern and southern parts of Zagros, which is consistent with the results of

similar research in the past (Lee et al. 2017; Potop and Mozny 2011; Stagge et al. 2015). In this study, SPEI predicted a higher relative frequency for dry conditions compared to SPI, this difference can be attributed to the sensitivity of SPEI to changes in precipitation and the inclusion of temperature parameters in this index which is consistent with (Polemio and Casarano 2008; Haile et al. 2020; Lweendo et al. 2017).

Evaluating the performance of GCMs and simulating future rainfall is important to understand current climate change and its impact on hydrology, water resources, agriculture, and ecology. We found that droughts will become more frequent in the Zagros region by 2100, which aligns with past studies (Rascon et al. 2021; Goodarzi et al. 2019; Lee et al. 2017; Haile et al. 2020; Bak and Kubiak-Wojcicka 2017; Lweendo et al. 2017; Shao et al. 2018; Yao et al. 2018). The results of this study can provide valuable input for further studies focusing on the whole country. In addition, future studies should employ several methods for combining GCMs to reduce the uncertainty associated with the predictions.

One of the most prominent features of this research is the joint implementation of models to predict the geographical and temporal extent of droughts in a semi-humid area. The use of other drought indicators along with other GCMs can be considered in future research. Also, the development of a network of stations measuring climate parameters could improve the accuracy, reliability, and coherence of predictions. Based on the results, it is expected that the range of areas affected by drought in the developed region will be necessary, therefore, it is necessary to make the arrangements and flexibility of the community-based in this region. These predictions can be considered for the formulation of adaptation strategies in the face of drought. The results of this research can be used to manage drought risk in the region and to coherently develop water and water supply development projects. These results are strongly dependent on simulations from only one set of climate change data. There are therefore limitations due to the uncertainty in various climate change scenarios. However, this study showed that the Zagros region will be exposed to significant drought due to climate change.

Declarations

Acknowledgments

We would like to express our gratitude toward those who helped us by providing data or improving our analyses.

Author's Contributions

All authors contributed to the study conception and design. Material preparation, data collection and analysis were performed by Mahsa Pakdin, Morteza Akbari and Mohamad Alizadeh Noughani. The first draft of the manuscript was written by Mahsa Pakdin and all authors commented on previous versions of the manuscript. All authors read and approved the final manuscript.

Data and Code availability

Please contact the corresponding author for data requests.

Ethics approval and consent to participate

Not applicable

Consent for publication

Authors have agreed to submit this manuscript in its current form for publication in the journal.

Competing interests

The authors declare no conflicts of interest.

Funding

No funding was received for conducting this study.

Corresponding Author Dr. Mahsa Pakdin.

References

1. Abbasi A, Khalili K, Behmanesh J, Shirzad A (2019) Drought monitoring and prediction using SPEI index and gene expression programming model in the west of Urmia Lake. Theor Appl Climatol 138:553–567. https://doi.org/10.1007/s00704-019-02825-9
2. Akbari M, Ownegh M, Asgari H, Sadoddin A, Khosravi H (2016) Drought Monitoring Based on the SPI and RDI Indices under Climate Change Scenarios (Case Study: Semi-Arid Areas of West Golestan Province). Ecopersia 4(4):1585–1602
3. Bak B, KubiakWojcicka K (2017) Impact of meteorological drought on hydrological drought in Toruń (central Poland) in the period of 1971–2015. Journal of Water and Land Development No. 32 p. 3–12. https://doi.org10.1515/jwld-2017-0001
4. Caccamo G, Chisholm L, Bradstock RA, Puotinen M (2011) Assessing the sensitivity of MODIS to monitor drought in high biomass ecosystems. Remote Sens Environ 115(10):2626–2639. https://doi.org/10.1016/j.rse.2011.05.018
5. Chanapathi T, Thatikonda S (2020) Investigating the impact of climate and land-use land cover changes on hydrological predictions over the Krishna River basin under present and future scenarios. Sci Total Environ 721:137736. https://doi.org/10.1016/j.scitotenv.2020.137736
6. Chen H, Sun J (2015) Changes in drought characteristics over China using the standardized precipitation evapotranspiration index. J Clim 28:5430–5447. https://doi.org/10.1175/JCLI-D-14-00707.1
7. Dubrovsky M, Svoboda M, Trnka M, Hayes M, Wilhite DA, Zalud Z, Hlavinka P (2008) Application of relative drought indices in assessing climate-change impacts on drought conditions in Czechia. Theor Appl Climatol 96:155–171. https://doi.org/10.1007/s00704-008-0020-x
8. Fang G, Yang J, Chen Y, Li Z, Maeyer P (2018) Impact of GCM structure uncertainty on hydrological processes in an arid area of China. Hydrol Res 49(3):893–907. https://doi.org/10.2166/nh.2017.227
9. Fathizadeh O, Attarod P, Pypker TG, Darvishsefat AA, Zahedi Amiri G (2013) Seasonal Variability of Rainfall Interception and Canopy Storage Capacity Measured under Individual Oak (Quercus brantii) Trees in Western Iran. Journal of Agricultural Science and Technology 15(1):175–188. http://jast.modares.ac.ir/article-23-4073-en.html
10. Fathian F, Ghadami M, Haghighi P, Amini M, Naderi S, Ghaedi Z (2020) Assessment of changes in climate extremes of temperature and precipitation over Iran. Theoret Appl Climatol. https://doi.org/10.1007/s00704-020-03269-2

11. Gebrewahid MG, Kasa AK, Gebrehiwot KA (2017) A.G.B Analyzing Drought Conditions, Interventions and Mapping of Vulnerable Areas Using NDVI and SPI Indices in Eastern Ethiopia, Somali Region. Ethiop. J. Environ. Stud. Manag. 10, 1137–1150. https://ejesm.org/doi/v10i9.3
12. Goodarzi M, Pourhashemi M, Azizi Z (2019) Investigation on Zagros forests cover changes under the recent droughts using satellite imagery. Jornal of Forest Science 65:9–17. https://doi.org/10.17221/61/2018-JFS
13. Haile G, Tang Q, Leng G, Jia G, Wang J, Cai D et al (2020) Long-term spatiotemporal variation of drought patterns over the Greater Horn of Africa. Sci Total Environ 704:135299. https://doi.org/10.1016/j.scitotenv.2019.135299
14. Hessl AE, Anchukaitis KJ, Jelsema C, Cook B, Byambasuren O, Leland C, Nachin B, Pederson N, Tian H, Hayles LA (2018) Past and future drought in Mongolia. Sci Adv 4(3):e1701832. https://doi.org/10.1126/sciadv.1701832
15. Huang YF, Ang J, Tiong Y, Mirzaei M, Mat Amin M (2016) Drought forecasting using SPI and EDI under RCP-8.5 climate change scenarios for Langat River Basin, Malaysia. Procedia Eng 154:710–717. https://doi.org/10.1016/j.proeng.2016.07.573
16. Solomon SD, Qin M, Manning Z, Chen M, Marquis K, Averyt M, Tignor M, Miller HL (2007) IPCC 2007 Climate change the physical science basis. Contribution of Working Group, I to the Fourth Assessment Report of the Intergovernmental Panel on Climate Change. Cambridge University Press, Cambridge, UK. and New York, NY, USA, p 996
17. IPCC (2013) Contribution of working group I to the fifth assessment report of the intergovernmental panel on climate change. In: Stocker TF, Qin D, Plattner G-K, Tignor M, Allen SK, Boschung J, Nauels A, Xia Y, Bex V, Midgley PM (eds) Climate Change 2013 The physical science basis.Cambridge University Press, Cambridge
18. Kang S, Zhang Q, Qian Y, Ji Z, Li C, Cong Z, Zhang Y, Guo J, Du W, Huang J, You Q, Panday AK, Rupakheti M, Chen D, Gustafsson O, Thiemans M, Qin D (2019) Linking atmospheric pollution to cryosphere change in the Third Pole region: current progress and future prospects. Nat Sci Rev 6(4):796–809. https://doi.org/10.1016/j.gsf.2021.101251
19. Khan M, Coulibaly P, Dibike Y (2006) Uncertainty analysis of statistical downscaling methods. J Hydrol 319(1–4):357–382. https://doi.org/10.1016/j.jhydrol.2005.06.035
20. Lin H, Wang J, Li F, Xie Y, Jiang C, Sun L (2020) Drought Trends and the Extreme Drought Frequency and Characteristics under Climate Change Based on SPI and HI in the Upper and Middle Reaches of the Huai River Basin, China. Water 12:1100. https://doi.org/10.3390/w12041100
21. Lee S, Yoo S, Choi J, Bae S (2017) Assessment of the Impact of Climate Change on Drought Characteristics in the Hwanghae Plain, North Korea Using Time Series SPI and SPEI: 1981–2100. Water 9(8). https://doi.org/10.3390/w9080579
22. Lweendo MK, Lu B, Wang M, Zhang H, Xu W (2017) Characterization of droughts in humid subtropical region, upper Kafue River basin (southern Africa). Water 9(4):242. https://doi.org/10.3390/w9040242
23. Mavromatis T (2007) Drought index evaluation for assessing future wheat production in Greece. International Journal of Climatology A J Royal Meteorologic Soc 27(7):911–924. https://doi.org/10.1002/joc.1444
24. Mirzayi Hasanlo A, Abghari H, Erfanian M, Choobe S (2020) An Assessment of Spatial and Temporal Changes in Precipitation and Drought in Iranian Synoptic Stations of Iran. Watershed Management Research Journal 33(4):126–144. https://doi.org/10.22092/wmej.2020.341216.1298

25. McKee TB (1995) Drought monitoring with multiple time scales. Proceedings of 9th Conference on Applied Climatology, Boston, 1995
26. Mehr A, Vaheddoost B (2019) Identification of the trends associated with the SPI and SPEI indices across. Ankara, Turkey. Theor Appl Climatol 139:1531–1542. https://doi.org/10.1007/s00704-019-03071-9
27. Memarian H, Akbari M (2021) Prediction of combined effect of climate and land use changes on soil erosion in Iran using GloSEM data. Iranian journal of Ecohydrology 8(2):513–534. https://doi.org/10.22059/ije.2021.320754.1482
28. Miao C, Duan Q, Sun Q, Huang Y, Kong D, Yang T et al (2014) Assessment of CMIP5 climate models and projected temperature changes over Northern Eurasia. Environ Res Lett 9:055007. https://doi.org/10.1088/1748-9326/9/5/055007
29. Mukherjee S, Mishra A, Trenberth KE (2018) Climate change and drought: a perspective on drought indices. Curr Clim Change Reports 4(2):145–163
30. Muhlenstadt T, Kuhnt S (2011) Kernal Interpolation. Computational Statistics and Data Analysis Elsevier, vol. 55(11), pages 2962-2974
31. Nabaei S, Sharafati A, Yaseen ZM, Shahid S (2019) Copula based assessment of meteorological drought characteristics: regional investigation of Iran. Agric For Meteorol 276–277:107611. https://doi.org/10.1016/j. agrformet. 06.010
32. Pakdin M, Akbari M, Alizadeh M (2021) Impacts of climate change on rangelands vegetation under different climate scenarios in Iran, The 1st International and the 8th National Conference on Rangeland Management, Iran. https://profdoc.um.ac.ir/paper-abstract-1085685.html
33. Paulo A, Rosa RD, Pereira L (2012) Climate trends and behavior of drought indices based on precipitation and evapotranspiration in Portugal. Natural Hazards Earth System Science 12:1481–1491
34. Zhifang P, Fang S, Wang L, Yang W (2020) Comparative Analysis of Drought Indicated by the SPI and SPEI at Various Timescales in Inner Mongolia, China. Water 12)7(: 1925. https://doi.org/10.3390/w12071925
35. Polemio M, Casarano D (2008) Climate change, drought and groundwater availability in southern Italy. Geological Society, London, Special Publications 288(1): 39–51
36. Potop V, Možný M (2011) The application a new drought index–Standardized precipitation evapotranspiration index in the Czech Republic. Mikroklima a mezoklima krajinných structur an antropogenních prostředí, 2(4), pp.1-12. ISBN 978-80-86690-87-2
37. Rascón J, Gosgot Angeles W, Quiñones Huatangari L, Oliva M, Barrena Gurbillón M (2021) Dry and Wet Events in Andean Populations of Northern Peru: A Case Study of Chachapoyas, Peru. Frontiers in Environmental Science 9(March):1–13. https://doi.org/10.3389/fenvs.2021.614438
38. Ren G, Ding Y, Zhao Z, Zheng J, Wu T, Tang G, Xu Y (2012) Recent progress in studies of climate change in China. Adv Atmos Sci 29:958–977
39. Shao D, Chen S, Tan X, Gu W (2018) Drought characteristics over China during 1980–2015. Int J Clamato 38:3532–3545
40. Singh B, Narang MP (1993) Indigestible cell wall fractions in relation to lignin content of various forages. Indian Journal of Animal Sciences 63 (2): 196-200. Available at: https://www.feedipedia.org/node/14762
41. Shiravand H, Hosseini SA (2020) A new evaluation of the influence of climate change on Zagros oak forest dieback in Iran. Theor Appl Climatol 141:685–697. https://doi.org/10.1007/s00704-020-03226-z

42. Semenov MA (2009) The use of multi-model ensembles from global climate models for impact assessment of climate change. EGU General Assembly Conference Abstracts 12732
43. Semenov Mikhail A, Stratonovitch P (2010) Use of multi-model ensembles from global climate models for assessment of climate change impacts. Climate Res 41(1):1–14. https://doi.org/10.3354/cr00836
44. Stagge JH, Tallaksen L, Gudmundsson L, Van Loon A, Stahl K (2015) Candidate distributions for climatological drought indices (SPI and SPEI). Int J Climatol 35(13):4027–4040
45. Tang Q (2020) Global change hydrology: Terrestrial water cycle and global change. Science China Earth Sciences 63(3):459–462
46. Taxak A, Murumkar A, Arya D (2014) Long term spatial and temporal rainfall trends and homogeneity analysis in Wainganga basin, Central India. Weather and Climate Extremes 4:50–61
47. Tirivarombo S, Osupile D, Eliasson P (2018) Drought monitoring and analysis: Standardised Precipitation Evapotranspiration Index (SPEI) and Standardised Precipitation Index (SPI). Phys Chem Earth Parts A/B/C 106:1–10
48. Teuling A, Van Loon A, Seneviratne S, Lehner I, Aubinet M, Heinesch B, Spank U (2013) Evapotranspiration amplifies European summer drought. J Geophys Res lett 40(10):2071–2075. doi:10.1002/grl.50495
49. Van Pelt S, Swart R (2011) Climate change risk management in transnational river basins: the Rhine. Water Resour Manage 25(14):3837–3861. https://doi.org /10.1007/s11269-011-9891-1
50. Vicente Serrano SM, Beguería S, López-Moreno J (2010) A multiscalar drought index sensitive to global warming: the standardized precipitation evapotranspiration index. J Clim 23(7):1696–1718
51. Wilby R, Harris I (2006) A framework for assessing uncertainties in climate change impacts: Low-flow scenarios for the River Thames, UK. Water Resour Res 42(2). https://doi.org/10.1029/2005WR004065
52. Wang H, Rogers JC, Munroe DK (2015) Commonly used drought indices as indicators of soil moisture in China. J Hydrometeorol 16:1397–1408. https://doi.org/10.1175/JHM-D-14-0076.1
53. Wolf JF, Abatzoglou J (2011) The suitability of drought metrics historically and under climate change scenarios. In 47th Annual Water Resources Conference, Albuquerque, NM (pp. 7-10)
54. Xu L, Abbaszadeh P, Moradkhani H, Chen N, Zhang X (2020) Continental drought monitoring using satellite soil moisture, data assimilation and an integrated drought index. Remote Sens Environ 250:112028
55. Valavi R, Shafizadeh Moghadam H, Matkan A (2019) Modelling climate change effects on Zagros forests in Iran using individual and ensemble forecasting approaches. Theor Appl Climatol 137:1015–1025. https://doi.org/10.1007/s00704-018-2625-z
56. Yao N, Li Y, Lei T, Peng L (2018) Drought evolution, severity and trends in mainland China over 1961–2013. Sci Total Environ 616–617:73–89. https://doi.org/ 10.1016/j.scitotenv.2017.10.327
57. Won J, Jang S, Kim K, Kim S (2018) Applicability of the evaporative demand drought index. Korean Society of Hazard Mitigation 18(6):431–442. https://doi.org/10.1016/j.scitotenv.2020.140701
58. Zargar A, Sadiq R, Naser B, Khan F (2011) A review of drought indices. Environ Re 19:333–349
59. Zhou B, Wen QH, Xu Y, Song L, Zhang X (2014) Projected changes in temperature and precipitation extremes in China by the CMIP5 multimodel ensembles. J Clim 27(17):6591–6611. https://doi.org/10.1175/JCLI-D-13-00761.1
60. Zhao H, Gao G, An W, Zou X, Li H, Hou M (2015) Timescale differences between SC-PDSI and SPEI for drought monitoring in China. Phys Chem Earth 102:48. https://doi.org/10.1016/j.pce.2015.10.022

Figures

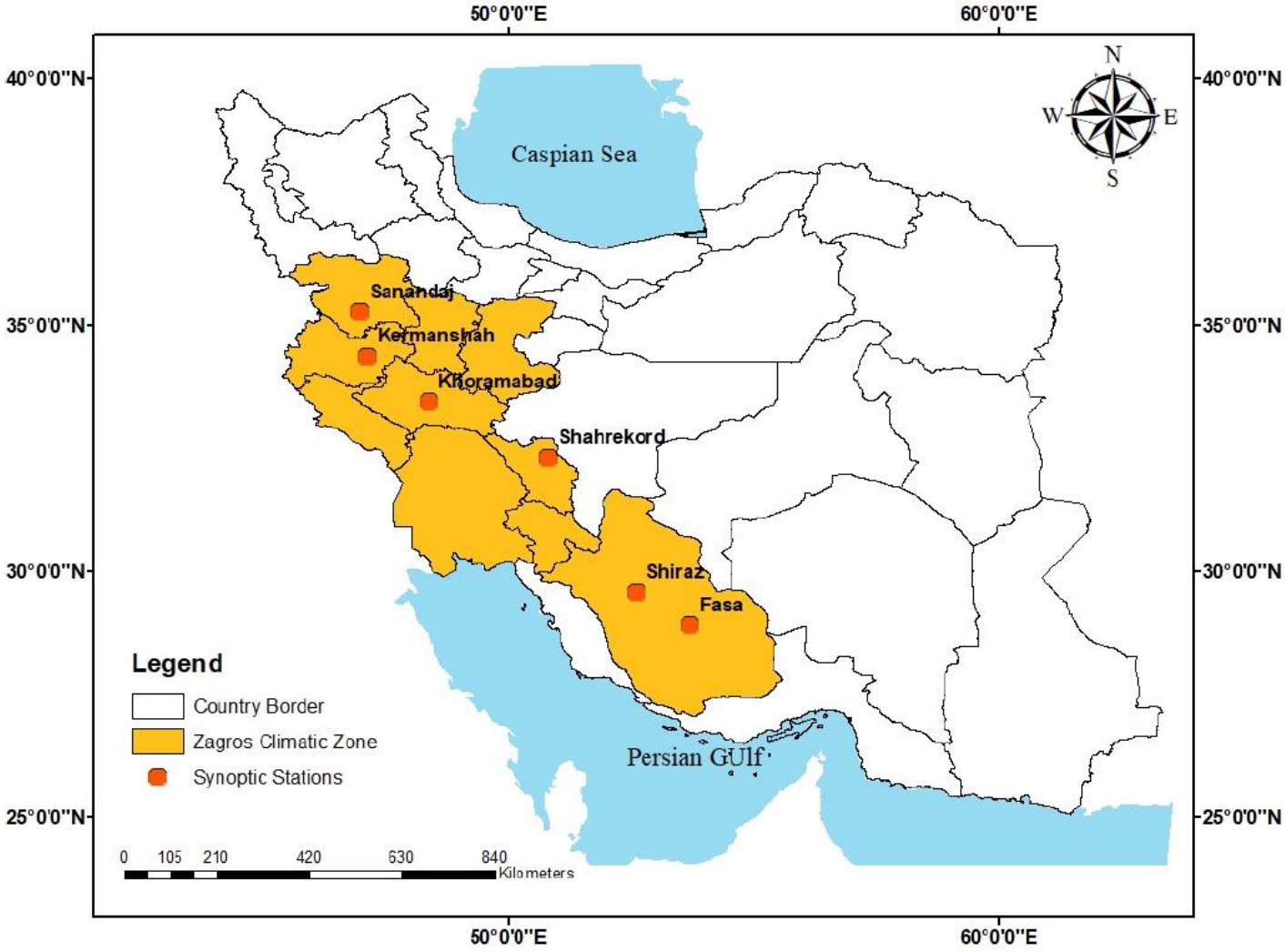

Figure 1

The location of the study area and the synoptic stations.

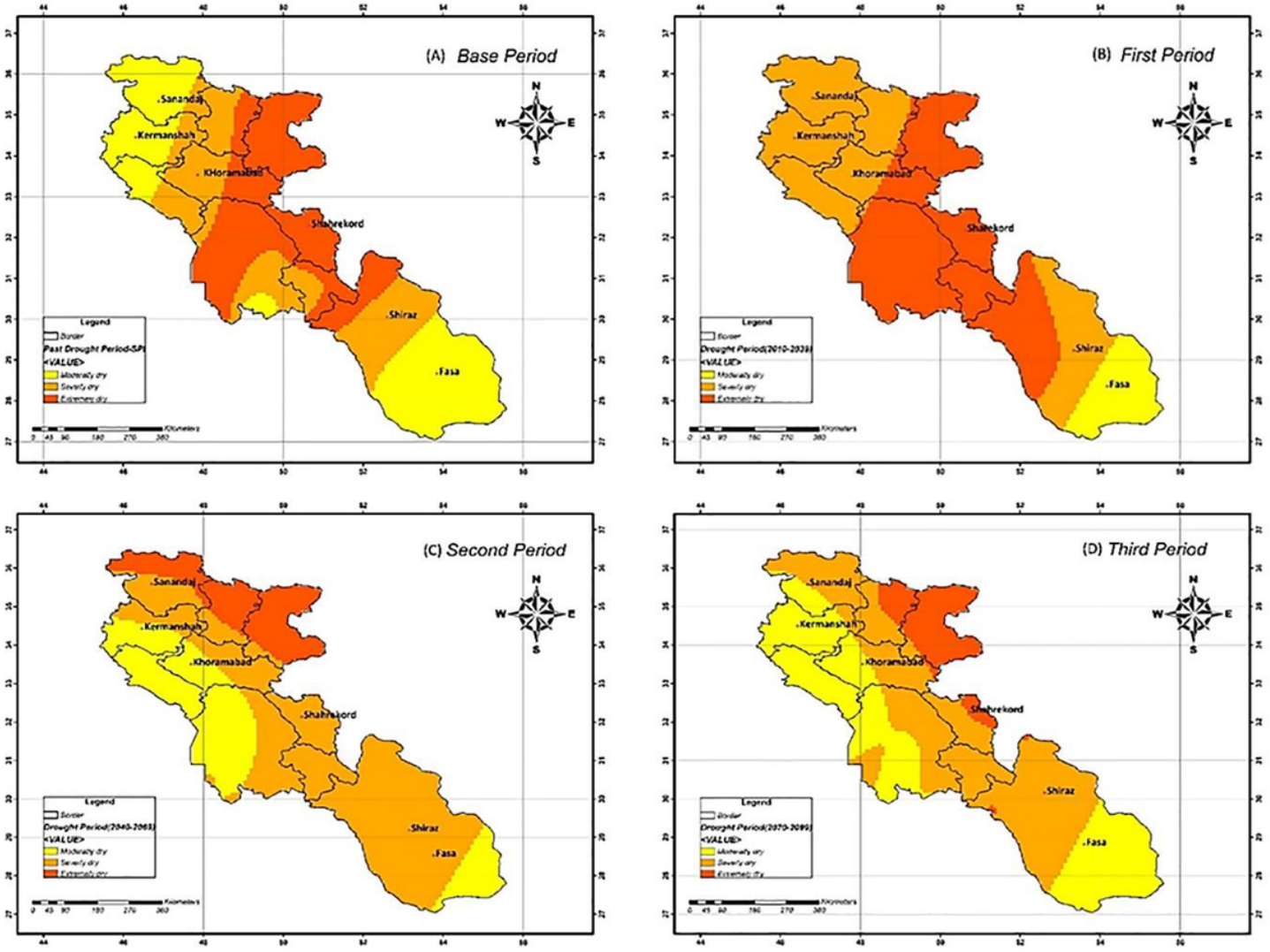

Figure 2

The spatial distribution of three classes of drought severity based on SPI during the base period (A), first period (B), the second period (C), and third period (D)

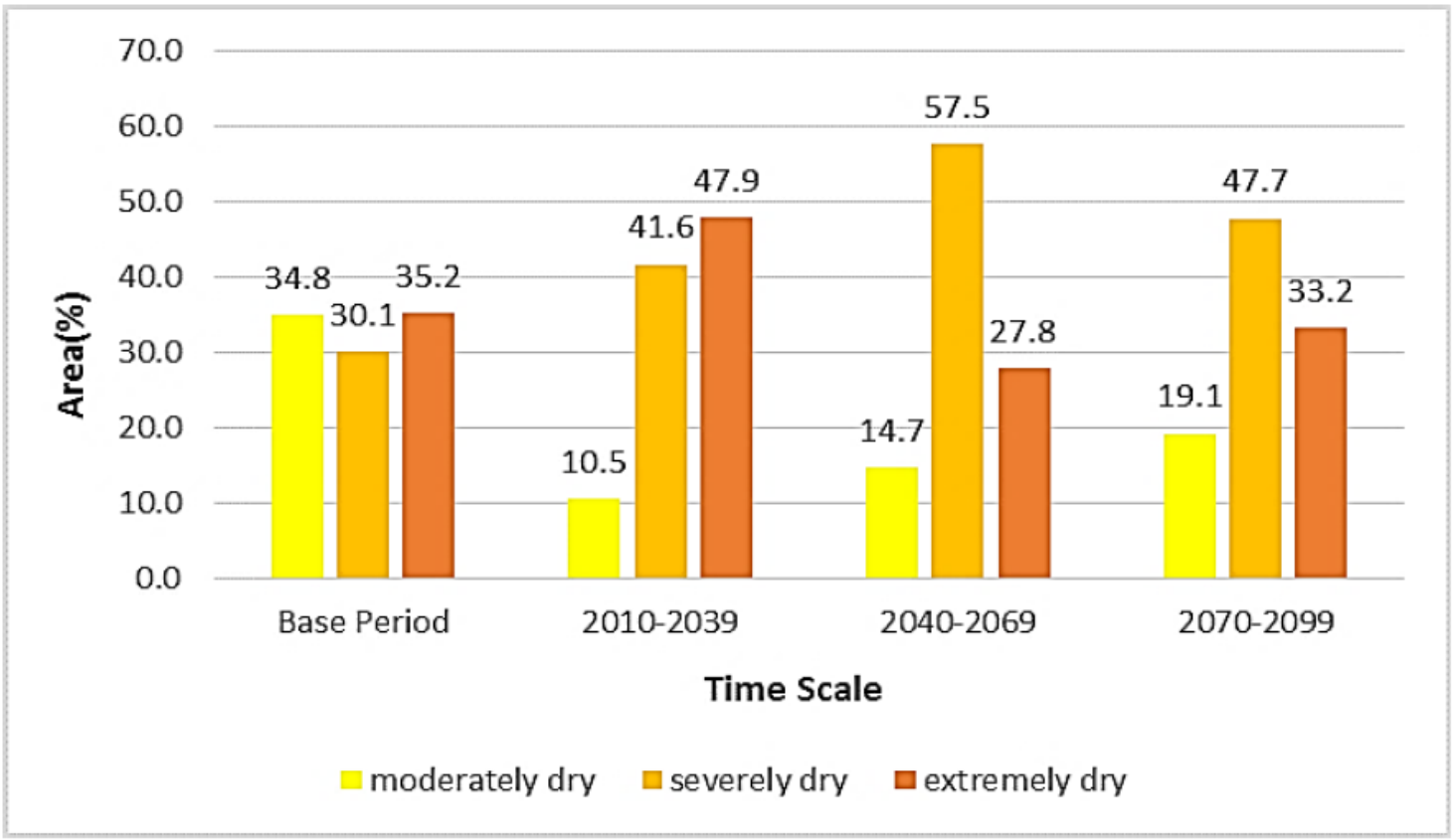

Figure 3

Percentage of drought severity classes in the past and future based on SPI

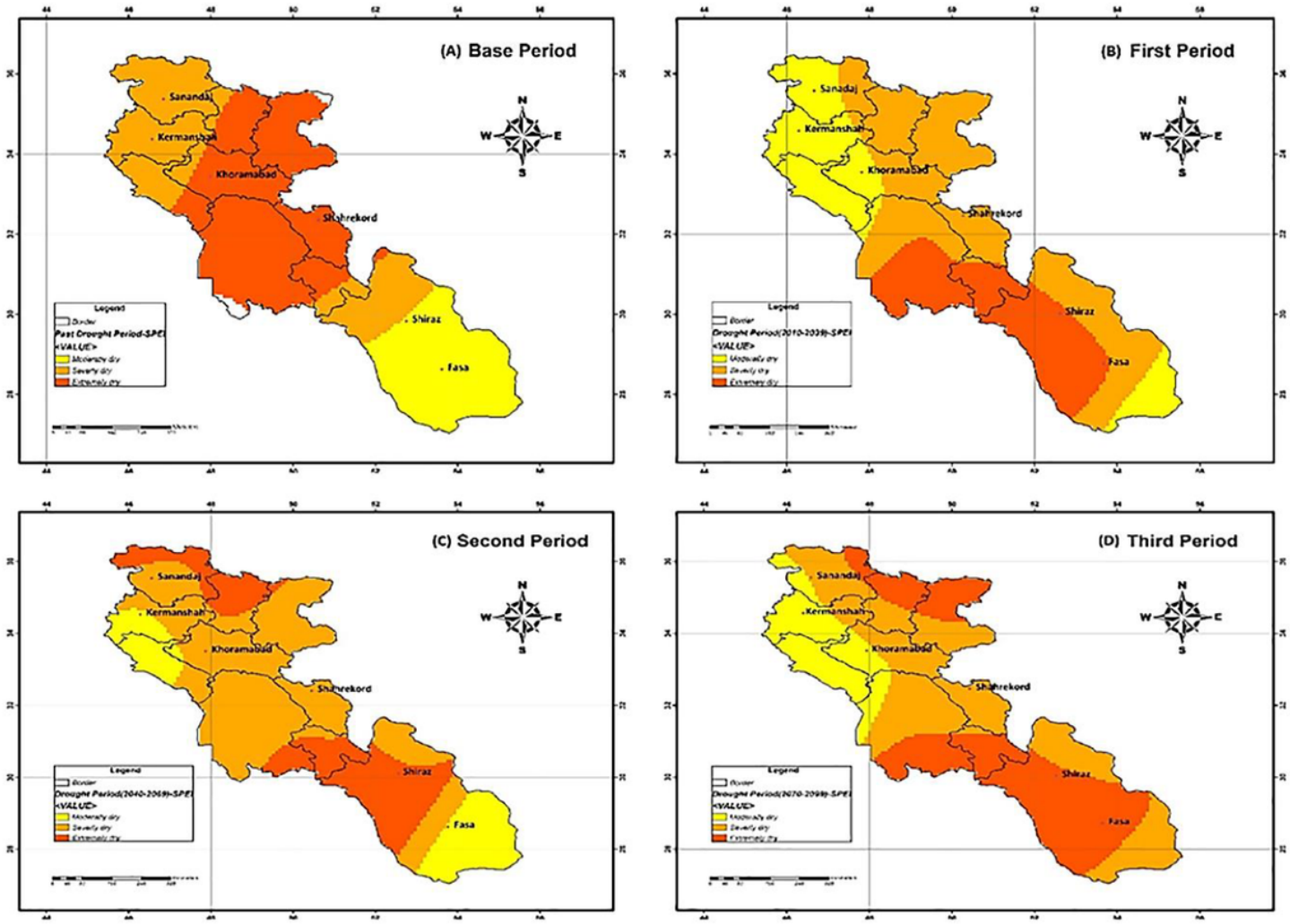

Figure 4

The spatial distribution of three classes of drought severity based on SPEI during the base period (A), first period (B), the second period (C), and third period (D)

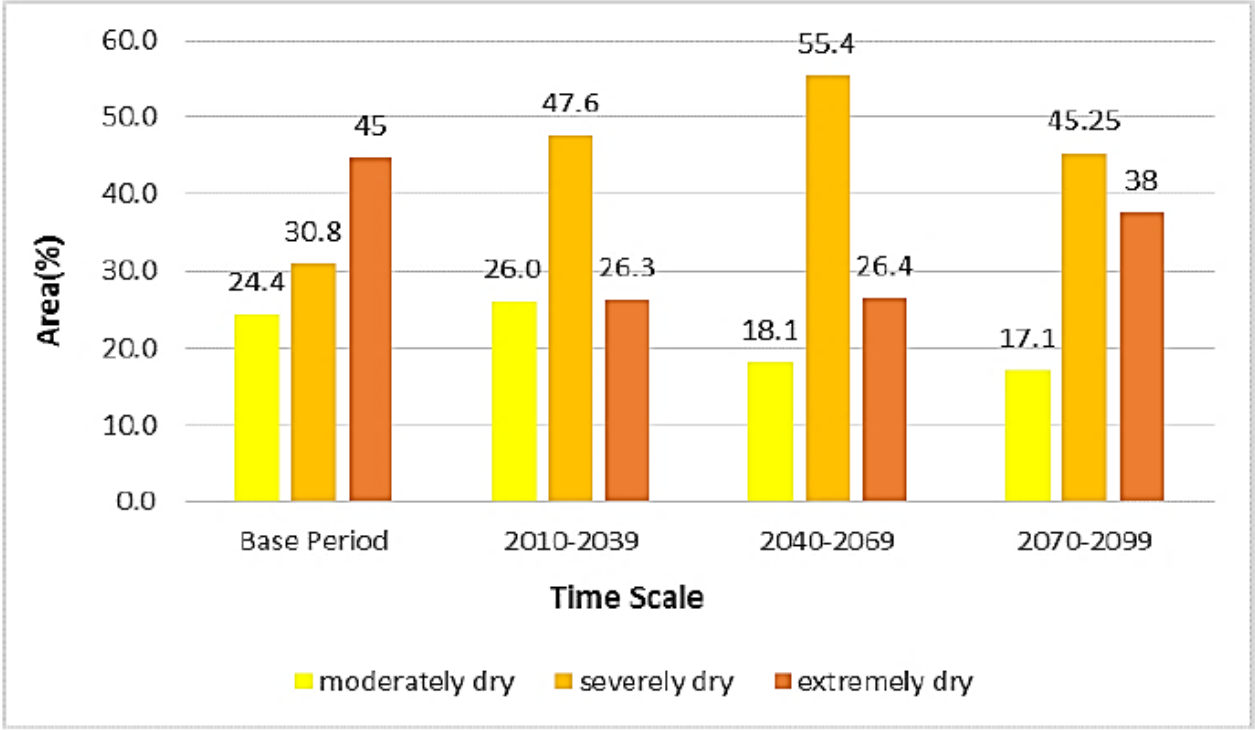

Figure 5

Percentage of drought severity classes in the past and future based on SPEI